Available online at www.sciencedirect.com
SCIENCE DIRECT
Polymer 46 (2005) 8045–8053
polymer
www.elsevier.com/locate/polymer

Basic and applied rheology of m-LLDPE/LDPE blends: Miscibility and processing features

R. Pérez[a], E. Rojo[a,*], M. Fernández[a], V. Leal[b], P. Lafuente[b], A. Santamaría[a]

[a]*Department of Polymer Science and Technology, POLYMAT, Faculty of Chemistry, University of the Basque Country, P.O. Box 1072, E-20080 San Sebastián, Spain*
[b]*Centro de Tecnología REPSOL-YPF, Ctra. N-V, Km 18, 28931 Móstoles, Madrid, Spain*

Received 3 December 2004; received in revised form 10 May 2005; accepted 9 June 2005
Available online 19 July 2005

Abstract

The linear viscosity of m-LLDPE/LDPE blends is adjusted to a free volume model, conceived for miscible blends. A deviation from the model is observed at 47.5% m-LLDPE/52.5% LDPE blend, suggesting immiscibility in the molten state at this composition. Time–temperature superposition method is used to confirm miscible and immiscible cases. The effect of miscibility on practical rheological features is analysed using extrusion rheometry. The results indicate a core-sheet morphology in the immiscible blend, as the less viscous LDPE encircles the m-LLDPE phase. Miscible blends with a high LDPE content and immiscible 47.5% m-LLDPE/52.5% LDPE blend, show 'melt fracture', but not 'sharkskin'. The latter is observed in miscible blends of a high m-LLDPE content. 'Sharkskin' is postponed in 87.5% m-LLDPE/12.5% LDPE blend, a result which is associated to the elongational viscosity enhancement, due to the presence of long chain branches. The correlation between melt spinning and blown film extrusion results is investigated, showing evidences of the technical limitations caused by immiscibilty.

Keywords: Metallocene polyethyelene blends; Rheology of polyethylene blends; Miscibility of metallocene polyethylenes

1. Introduction

The recent use of metallocene or single-site catalysts to obtain polyethylenes with narrow molecular weight distributions has opened new possibilities for polyethylene blends. But still the number of papers dealing with blends based on metallocene catalyzed polyethylenes is limited. Several years ago the rheological behavior of metallocene catalysed high density polyethylene blends was investigated by our group [1]. More recently, the rheological features and miscibility of metallocene based linear low density polyethylene (m-LLDPE) and low density polyethylene (LDPE) blends have been published [2–8]. In these papers, linear dynamic viscoelastic results are reported, with the aim of investigate miscibility in the molten state. Yamaguchi and Abe [2] use time–temperature results to conclude that m-LLDPE and LDPE are miscible in the molten state at all blend compositions. The same conclusion is reached by Kwag et al. [8], using Cole Cole plots as miscibility criterium. In the same sense, Xu et al. [4] assume that the positive deviation of the linear viscosity, η_0, from the logarithmic additivity rule, in plots of η_0 vs. blend composition, indicates an immiscible state of blend melts. However, using dynamic viscoelastic results Hussein et al. [5–7], conclude that miscibility depends on short chain branch (SCB) content of m-LLDPE. According to these authors, molten blends of m-LLDPE with LDPE are miscible in the LLDPE branching range 10–30 branches/1000C. Small-angle neutron scattering (SANS) and spectroscopic studies on blends of conventional (Ziegler Natta) LLDPEs with deuterated HDPEs, reveal also the role played by SCB in molten state miscibility [9–12]. In particular Tashiro and Gose [12] observe that the blend which contains a LLDPE with 17 ethyl branches per 1000 carbon atoms is homogeneous, but the blend containing a LLDPE with 41 ethyl branches is heterogeneous.

On the other hand, very few papers refer to the applied rheology related to processing of m-LLDPE/LDPE blends

* Corresponding author. Tel.: +34 943 018184; fax: +34 943 015270.
E-mail address: pobveboj@sc.ehu.es (E. Rojo).

0032-3861/$ - see front matter © 2005 Elsevier Ltd. All rights reserved.
doi:10.1016/j.polymer.2005.06.087

[8,13–14]. In particular Ajji et al. [14] investigate the relevance of elongational viscosity to the film blowing process of these blends.

To cover this gap, novel basic and applied rheological results of blends of a metallocene catalysed m-LLDPE with LDPE are presented in this paper. The work is organized as follows. The Newtonian or linear viscosity η_0 of the blends, obtained from dynamic viscoelastic measurements, is adjusted to a free volume model conceived for miscible systems. Time–temperature superposition method is used to confirm the miscibility and the immiscibility of the considered blend compositions. The effect of miscibility on practical rheological features associated to processing methods is investigated through extrusion capillary measurements, focusing on surface distortions. Melt spinning experiments are accomplished to justify the flow instability results, in particular the shift to high shear rates found for the onset of 'sharkskin' in 87.5% m-LLDPE/12.5% LDPE blend. Finally, a possible correlation between melt spinning results and the capability of the blends to blown film extrusion is investigated.

2. Experimental section

2.1. Materials and blends preparation

The molecular parameters of a prototype pure m-LLDPE made by Repsol-YPF and a commercial LDPE sample (Repsol-YPF) are shown in Table 1. Blends of both samples were prepared in a twin screw extruder, at the compositions indicated in the text; stabilizers and processing aid additives were also mixed during blend preparation.

2.2. Dynamic viscoelastic measurements

The viscoelastic functions were determined in a ARES rheometrics scientific rheometer operating in the oscillatory shear mode, using parallel plates geometry with $d=25$ mm, in a frequency range of 10^{-2}–10 Hz and temperature range of 130–190 °C. All the data were obtained under linear viscoelastic conditions. Low frequency experiments, which involve long times, require using N_2 atmosphere to avoid degradation.

2.3. Extrusion capillary measurements

Capillary extrusion measurements were performed at 190 °C in a Göttfert Rheograph 2002 rheometer using a flat entry capillary tungsten die of 1 mm diameter and a *L/D* ratio of 30. The surface of extrudates was analyze by scanning electron microscopy with a Hitachi-2100 microscope, using an accelerating voltage of 15 kV.

2.4. Melt spinning

Samples were melt spun as monofilaments at 190 °C using a homemade melt spinning line. Extrudates obtained at $\dot{\gamma} = 36.1\ s^{-1}$ in the rheometer described above, were stretched with a rotor. The tensile force F was measured as the draw ratio v_1/v_0 (v_1 is the take up velocity at the rotor; v_0 is the velocity at the exit of the die) was increased up to filament rupture. The elongational stress σ_{11}, an apparent elongational strain $\dot{\varepsilon}_E$ rate and an apparent elongational viscosity η_E, were determined using the following equations:

$$\sigma_{11} = \frac{Fv_1}{s_0 v_0} \tag{1}$$

$$\dot{\varepsilon}_E = \frac{v_1 - v_0}{L} \tag{2}$$

$$\eta_E = \frac{\sigma_{11}}{\dot{\varepsilon}_E} \tag{3}$$

where s_0 is the cross-section of the die and L the distance between the die and the rotor.

Eq. (2) results from a linear increase of the velocity from the exit of the die to the rotor, which is a simplification of the exponential velocity profile considered in the literature [15]. This gives rise to an apparent elongational viscosity that we use for comparison purposes among the investigated samples.

2.5. Blown film extrusion

The experiments were carried out using a Collin laboratory film blowing line, equipped with a 30 mm diameter extruder and a spider die of 60 mm. The annular spider die-gap was 1.6 mm. All the samples were processed at a blown up ratio (BUR) of 2.5. The system was conditioned to process metallocene polyethylenes.

3. Results and discussion

3.1. Application of a free volume model to complex viscosity results

The real part of the complex viscosity, η', of the

Table 1
Molecular characteristics of the polyethylenes used to prepare the blends

m-LLDPE/LDPE	M_n (g/mol)	M_w (g/mol)	M_w/M_n	SCB/1000C	LCB/1000C
100/0	37,500	99,500	2.7	10.5	
0/100	17,000	114,000	6.7		4.25

investigated samples is presented in Fig. 1 as a function of frequency. Experimental data fit very well to the Carrreau–Yasuda [16] four parameter model:

$$\eta' = \eta_0[(1 + (\lambda\omega)^a]^{(n-1)/a} \quad (4)$$

where η_0 is the Newtonian or linear viscosity, λ is the relaxation time, n is the 'power-law exponent', which describes the slope of η' as it decreases with frequency, and a is a dimensionless parameter that describes the transition region between the linear region (defined by η_0) and the power law region. The inverse of the frequency or shear rate for the onset of non-linear behaviour, actually the relaxation time λ, is taken as the reptation time of the 'tube and reptation' model [17]. On the other hand, the parameter a is considered as indicative of the broadness of the spectrum of relaxation times: The greater the deviation from $a=1$ (which actually would correspond to the case of only one relaxation time) the broader the spectrum is [18]. The values of the four parameters, obtained for blends and pure polymers, are included in Table 2. Since it is assumed that reptation is considerably hindered when chains have long branches, the LCB effect is noticed by the high λ values found for LDPE and the blends of a high content of this polymer. This also forces each molecule to relax by different mechanisms, giving rise to a broad spectrum of relaxation times: The small values of the parameter a found for LDPE and the LDPE rich blends, reflect this broadening effect.

Considering that the SCB level of our m-LLDPE (Table 1) lies within the range prone to miscibility with LDPE (Section 1), we initially assume that our blends are miscible. This assumption allows us to apply a thermodynamical model based on the effect of the molecular

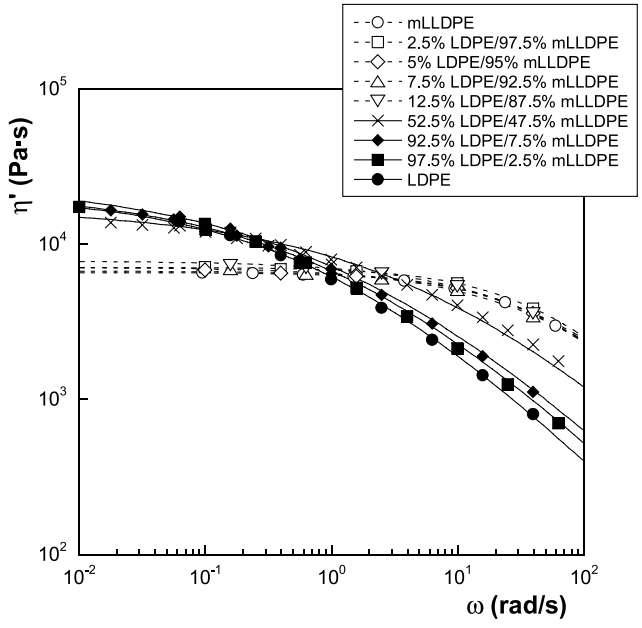

Fig. 1. The real part of the complex viscosity, η', of the investigated samples as a function of frequency, at a temperature $T=190$ °C.

Table 2
Parameters of Eq. (4), used to fit the dynamic viscosity data as a function of frequency

m-LLDPE/LDPE	η_0 (Pa s)	λ (s)	a
100/0	6575	0.021	0.82
97.5/2.5	7100	0.020	0.82
95/5	6700	0.020	0.80
92.5/7.5	7100	0.015	0.62
87.5/12.5	7800	0.016	0.60
47.5/52.5	18,000	0.097	0.37
7.5/92.5	26,000	0.60	0.38
2.5/97.5	23,000	0.76	0.42
0/100	21,000	0.97	0.46

A value of the 'power-law exponent' ($n=0.18$) is fixed for all the samples. The physical meaning of the parameters is given in the text.

weight and the free volume on the viscosity. Since this model is conveniently described in a previous paper [1], only the resulting equation for the viscosity of the blend, η_{0b}, is presented here:

$$\eta_{0b} = \left(\sum_i \Phi_i A_i (M)^{1/b}\right)^b \exp \frac{1}{\sum_i \Phi_i f_i + \prod_i K\Phi_i} \quad (5)$$

where ϕ_i and f_i are, respectively, the volume fraction and the free volume fraction of each blend component ($i=1, 2$), K is a constant which accounts for the modifications of the free volume of the blends due to the mixing process and b is the power law exponent of the scaling law $\eta_0 \propto M_w^b$. Generally a value $b=3.4$ is accepted. Free volume fractions of each component are determined assuming a linear variation with temperature [19], taking a glass transition temperature $T_g=200$ K for both polyethylenes and using the activation energies of flow $E_a=29$ kJ/mol and $E_a=46$ kJ/mol, for m-LLDPE and LDPE, respectively. The factor that includes the molecular weight effect A_i can be calculated assuming $(\eta_0)i=A_i(M)\exp(1/f_i)$.

Fig. 2 shows the data of the linear viscosity, η_0, plotted against the blend composition. As can be seen, the best fit of the model to our experimental data (with $K=0.01$ and $b=3.4$), gives good results for low concentrations blends. However, it is not able at all to approach to the viscosity value obtained experimentally for 47.5% m-LLDPE/52.5% LDPE blend. This result restricts our initial assumption of miscibility to certain blend compositions, excluding from miscibility blends of a composition close to 50/50. A similar conclusion was reached by Hussein et al. [6] for linear low density polyethylenes, with a short chain content 14.4 CH_3/1000C and LDPE blends.

3.2. Time–temperature superposition

Miscibility of polymer blends in the molten state has been much less studied than in the solid state. Certainly, miscibility criteria based on glass transition temperature are useless in molten blends. Other techniques like those

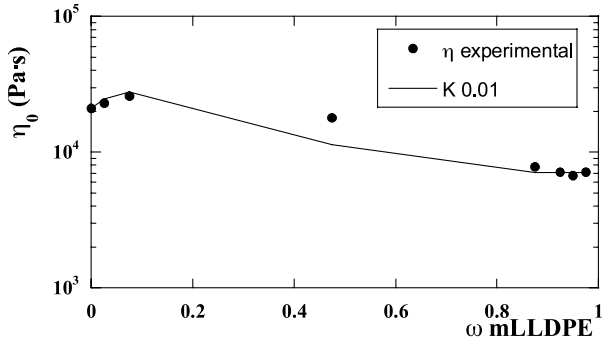

Fig. 2. Data of the linear viscosity, η_0, plotted against the blend composition. The best fit of the model is obtained with $K=0.01$ and $b=3.4$ (Eq. (5)). The experimental viscosity value of 47.5% m-LLDPE/52.5% LDPE blend is not adjusted by the model.

mentioned in Section 1, are therefore, necessary. The study of the dynamic viscoelastic functions at different temperatures and the associated analysis of the empirical principle of time–temperature superposition, have been employed to investigate miscibility and phase separation [20–33]. In the general field of complex liquids, like polymer blends, microphase-separated block copolymers, polymeric liquid crystals and others, two rheological methods have been revealed as particularly easy and suitable to analyze the validity of the time-superposition method: (a) log G' vs. log G'' plots, first proposed by Han and Lem [34] and (b) plots of phase angle δ vs. complex modulus G^*, proposed by Mavridis and Shroff [35]. Recently this last method has been used to investigate the presence of very small amounts of LCB in metallocene catalysed polyethylenes [36]. The encouraging results obtained in the characterization of the molecular architecture of polyethylenes, led us to use the plots proposed by Mavridis and Shroff to analyze our blends. Our analysis is based on an important discovery of these authors concerning time–temperature superposition in polyethylenes: HDPEs and other linear polyolefins require only a horizontal shift activation energy to superpose data, but long chain branched LDPEs require both horizontal and vertical activation energies. In Fig. 3 it is observed that a vertical shift has to be applied to superpose the loss tangent results obtained at different temperatures; vertical shifts are also necessary for 2.5% m-LLDPE/97.5% LDPE and 7.5% m-LLDPE/92.5% LDPE blends (not shown). However, in the case of m-LLDPE and its blends with low amounts of LDPE, direct superposition with no additional shift, is obtained in δ vs. G^* (Fig. 4). Miscible blends, dominated or not by LCB effects depending on LDPE content, can be assessed. But the most interesting, although not surprising, result concerns 47.5% m-LLDPE/52.5% LDPE blend, which is immiscible according to the results of Fig. 2. As can be seen in Fig. 5, it becomes impossible to apply any kind of shift to superpose data, since the form of the curves varies with frequency and temperature. This break of time–temperature superposition reflects the different relaxation times involved in phase separated linear and LCB chains.

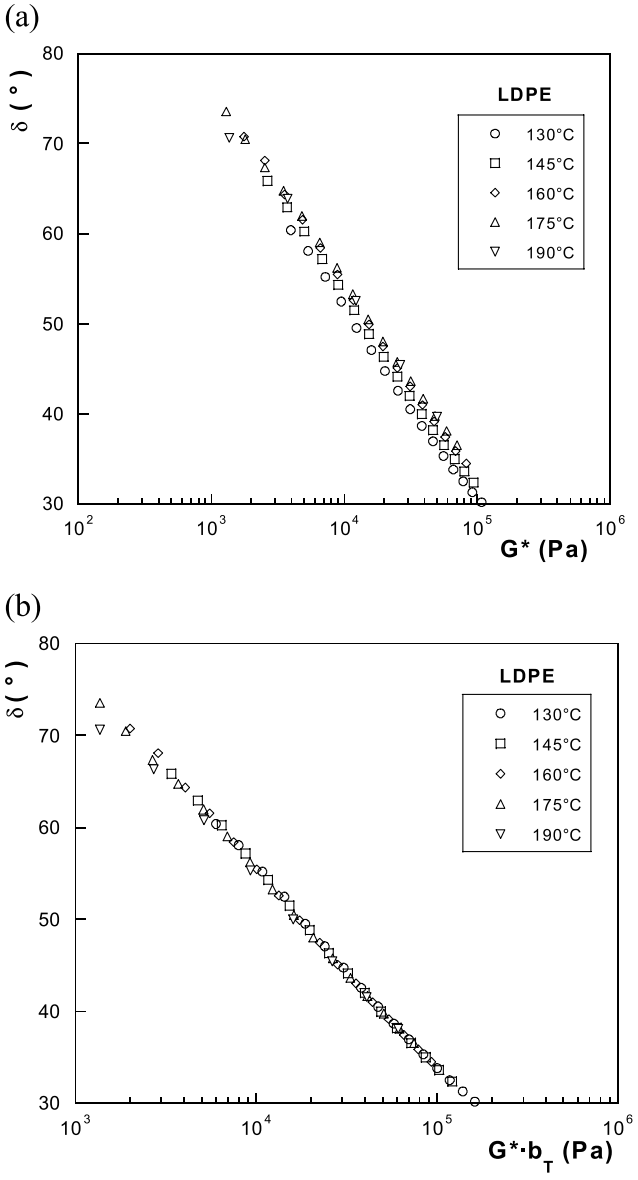

Fig. 3. (a) Plots of phase angle δ vs. complex modulus G^*, obtained at different frequencies and temperatures, for LDPE sample. (b) Plots of phase angle δ vs. complex modulus G^* with vertical shift factor, b_T, for LDPE sample.

Other rheological results, which are presented and discussed below, indicate that this blend is a two phase system where LDPE constitutes the continuous phase.

3.3. Extrusion capillary rheometry: Flow instabilities

A preliminary idea of the workability of our blends in industrial processes is given by flow curves, which have been obtained with a capillary rheometer at shear rates ranging from 5 to 1500 s^{-1}. Some of the results are presented in Fig. 6. As it could be expected considering its more shear thinning behavior, LDPE displays a lower viscosity in steady shear flow experiments. This is a significant result, since it indicates that at the shear rates

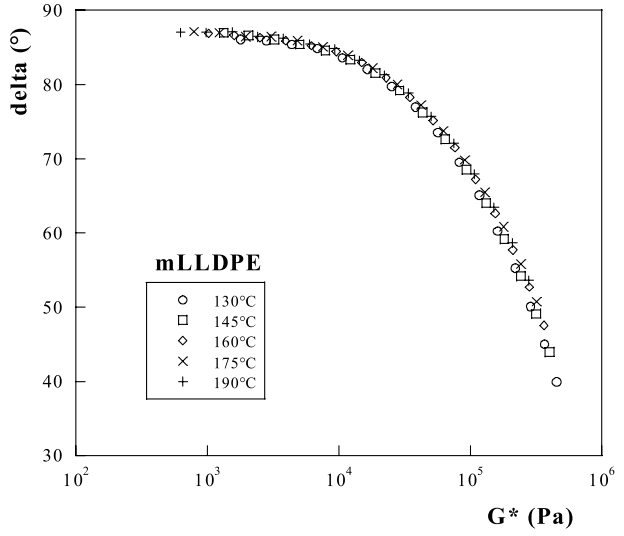

Fig. 4. Plots of phase angle δ vs. complex modulus G^*, obtained at different frequencies and temperatures, for m-LLDPE sample. Same behaviour is observed for blends of a high m-LLDPE content.

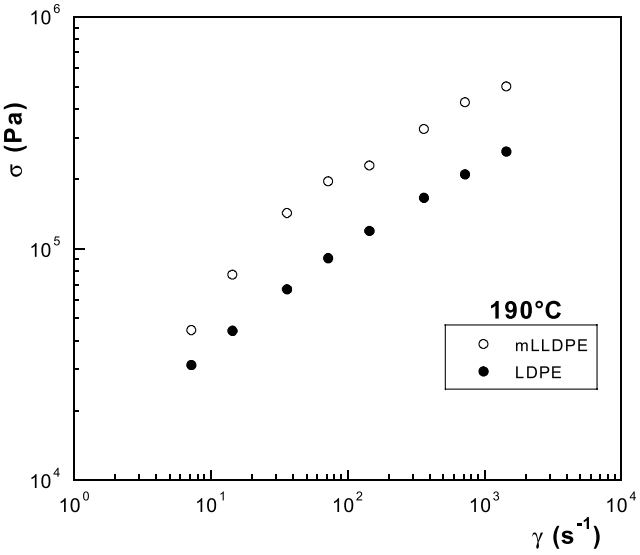

Fig. 6. Flow curves of the pure materials obtained with a capillary extrusion rheometer at 190 °C. Table 3 depicts the observed instabilities.

developed during mixing of immiscible 47.5% m-LLDPE/52.5% LDPE blend, LDPE will constitute the continuous phase, owing to its lower viscosity. The effect of this two phase morphology, characterized by a surrounding LDPE phase, is noted in flow instabilities, as well as in melt spinning results.

Three types of flow instabilities have been detected in the extrudates obtained with our samples: Besides the well known 'sharkskin' and 'melt fracture' effects, another surface irregularity, that we call 'striped extrudate' is observed. This surface irregularity, shown in Fig. 7, appears as a peculiarity of LDPE, which, as it is well known, also exhibits 'melt fracture', but not 'sharkskin'. A summary of the detected instabilities and their corresponding shear rates, is presented in Table 3. As expected, 2.5% m-LLDPE/97.5% LDPE and 7.5% m-LLDPE/92.5% LDPE miscible blends show the same features as LDPE. Interestingly enough, the 47.5% m-LLDPE/52.5% LDPE immiscible blend also displays 'striped extrudate' irregularity and 'melt fracture', but not 'sharkskin'. Therefore, as far as flow instabilities are concerned, this immiscible blend behaves like pure LDPE. This confirms the hypothesis that LDPE forms the continuous phase, wetting the capillary wall during flow and obliging the more viscous m-LLDPE to migrate to the center. What we define as 'striped extrudate' is actually a prelude to 'melt fracture', which it is known to be associated to a melt cracking provoked by a critical tensile stress at the entrance of the die. The high melt elasticity of LDPE, 2.5% m-LLDPE/97.5% LDPE, 7.5% m-LLDPE/92.5% LDPE and 47.5% m-LLDPE/52.5% LDPE samples, revealed by the large relaxation times

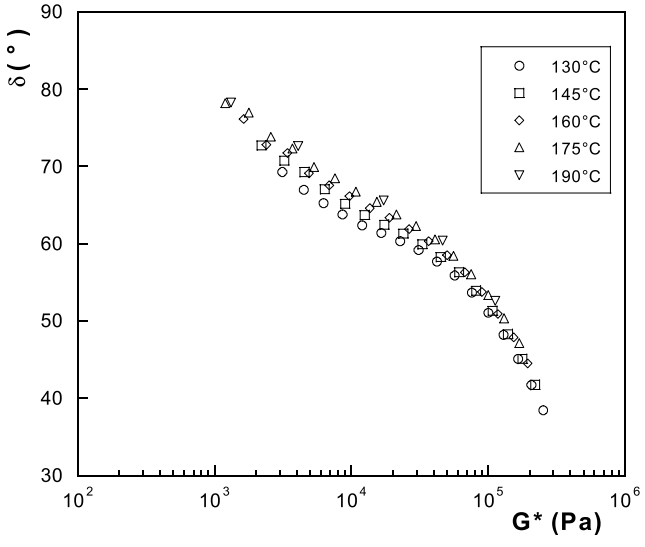

Fig. 5. Plots of phase angle δ vs. complex modulus G^*, obtained at different frequencies and temperatures, for 47.5% m-LLDPE/52.5% LDPE blend. Break of time–temperature superposition is observed.

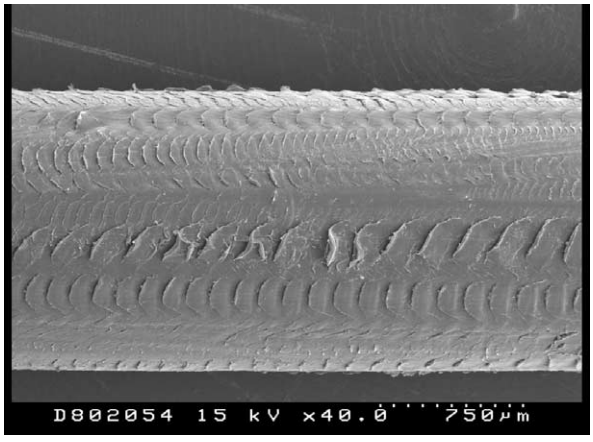

Fig. 7. A new surface irregularity, that we call 'striped extrudate', observed for LDPE and LDPE based blends (see text and Table 3).

Table 3
Observed flow instabilities, as shear rate is increased

m-LLDPE/LDPE	7.22 s^{-1}	14.44 s^{-1}	36.1 s^{-1}	72.2 s^{-1}	144.4 s^{-1}	361 s^{-1}	722 s^{-1}	1444 s^{-1}
100/0	Smooth	Smooth	Smooth	Ligth shark-skin	Ligth shark-skin	Smooth	Smooth	Fracture
95/5	Smooth	Smooth	Smooth	Ligth shark-skin	Ligth shark-skin	Ligth shark-skin	Fracture	Fracture
97.5/2.5	Smooth	Smooth	Smooth	Smooth	Ligth shark-skin	Ligth shark-skin	Fracture	Fracture
92.5/7.5	Smooth	Smooth	Smooth	Ligth shark-skin	Ligth shark-skin	Ligth shark-skin	Fracture	Fracture
87.5/12.5	Smooth	Smooth	Smooth	Smooth	Smooth	Smooth	Fracture	Fracture
47.5/52.5	Smooth	Smooth	Smooth	Striped	Striped	Fracture	Fracture	Fracture
7.5/92.5	Smooth	Smooth	Smooth	Smooth	Striped	Fracture	Fracture	Fracture
2.5/97.5	Smooth	Smooth	Smooth	Striped	Striped	Fracture	Fracture	Fracture
0/100	Smooth	Smooth	Smooth	Striped	Fracture	Fracture	Fracture	Fracture

The presence of processing aid additive reduces the amplitude of the extrudate roughness, but does not eliminate 'sharkskin' at the indicated shear rates.

(Table 2) associated to LCB, favors the development of 'melt fracture'.

'Sharkskin', which is typically observed for metallocene catalyzed m-LLDPEs, is also noticed for 97.5% m-LLDPE/2.5% LDPE, 95% m-LLDPE/5% LDPE and 92.5% m-LLDPE/7.5% LDPE blends. This is not a surprise at all, considering the dominating effect of m-LLDPE in these blends. However, the high shear rate found for the onset of 'sharkskin' in the case of 87.5% m-LLDPE/12.5% LDPE blend, is remarkable. Wider extrusion conditions can be envisaged for this blend, as compared with the other blends and pure polyethylenes: Smooth extrudates, without any kind of irregularty, can be obtained at least up to 361 s^{-1}.

The nowadays mostly accepted model for 'sharkskin' is based on the hypothesis, first suggested by Cogswell [37], that the extensional nature of the flow at the exit causes a tearing or cracking at the surface of the extrudate. Rutgers and Mackley [38], have presented a surface instability map where the onset of 'sharkskin' is correlated with the principal stress difference peak at the exit and the rupture stress of stretched molten fiber. A general conclusion extracted from this work is that 'sharkskin' is shifted to higher shear rates, as the measured 'melt stress' (stress at breakage determined in a melt spinning experiment) increases. On the other hand, Migler et al. [39,40] have disclosed the role played by the stretching rate just past the capillary exit, defining a critical reconfiguration rate parameter beyond which 'sharkskin' is observed. The 'reconfiguration rate' is given by:

$$\dot{T} = \frac{\dot{\varepsilon}(T+1)}{2} \tag{6}$$

where $\dot{T}$ and $\dot{\varepsilon}$ are, respectively, the deformation and the elongational strain rate in the immediate vicinity of the exit. Interestingly enough the authors note that sharkskin occurs for the same critical value of $\dot{T}$ under stick or slip boundary conditions.

On the basis of these works, we have tried to understand and justify the promising result obtained for our 87.5% m-LLDPE/12.5% LDPE blend (Table 3), investigating the elongational properties of our samples.

3.4. Melt spinning experiments: Correlation with 'sharkskin' and blown film extrusion

Elongational flow curves ($\log \sigma_{11}$ vs. $\log \dot{\varepsilon}$), determined using Eqs. (1) and (2), are shown in Fig. 8. From these plots an apparent elongational viscosity $\eta_E = \sigma_{11}/\dot{\varepsilon}_{11}$ can be obtained. Since data of Fig. 8 fit to straight lines, the determined elongational viscosity is constant (rate independent) for each sample; the values are given in Table 4. The maximum σ_{11} value obtained for each sample in Fig. 8 is the 'melt stress' or the stress at rupture of the melt, σ_M, under the conditions established in the experimental part. The LDPE sample, as well as miscible 2.5% m-LLDPE/97.5% LDPE, 7.5% m-LLDPE/92.5% LDPE and immiscible 47.5% m-LLDPE/52.5% LDPE blends, all of which show a similar behavior in flow instabilities analysis, also displays resembling elongational features, characterized by a low σ_M and high tensile viscosity. According to Wagner et al. [41], the stress at rupture of LDPE melts is of the same order of magnitude as the critical tension at the entrance of the die, beyond which 'melt fracture' is observed. Taking this into

Table 4
Rate independent apparent elongational viscosity (Section 2 and Fig. 8) of the analysed samples

m-LLDPE/LDPE	η_E (Pa s)
100/0	3.2×10^6
97.5/2.5	3.6×10^6
95/5	4.7×10^6
92.5/7.5	4.8×10^6
87.5/12.5	5.5×10^6
47.5/52.5	1.4×10^7
7.5/92.5	1.5×10^7
2.5/97.5	1.3×10^7
0/100	1.4×10^7

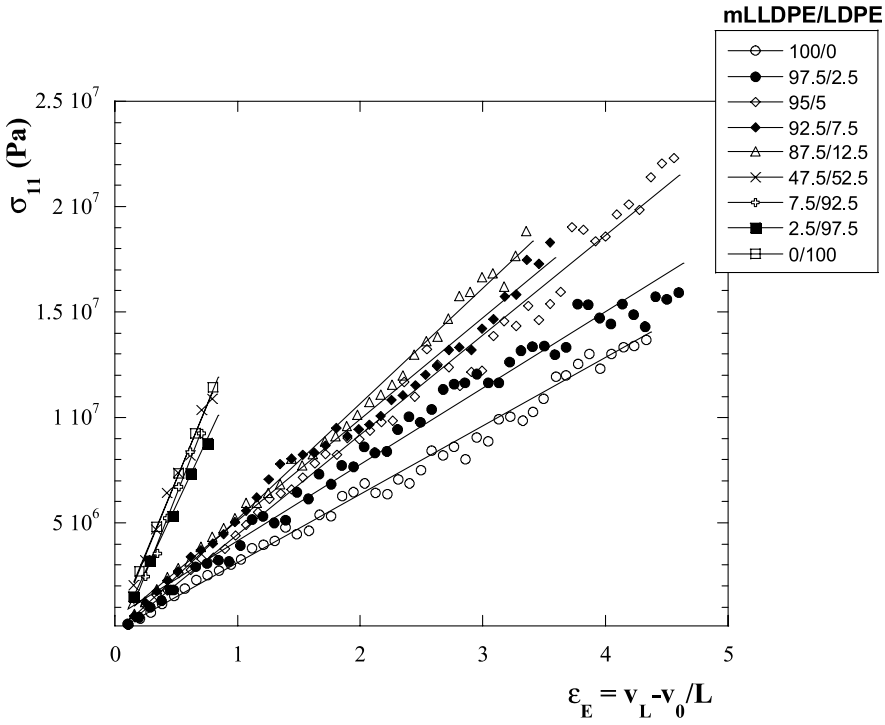

Fig. 8. Elongational flow curves (log σ_{11} vs. log $\dot{\varepsilon}$) of the investigated samples, determined using Eqs. (1) and (2). The maximum elongational stress value obtained for each sample is the 'melt stress' (see text).

account, no significant differences should be found for the onset of 'melt fracture' of LDPE, 2.5% m-LLDPE/97.5% LDPE, 7.5% m-LLDPE/92.5% LDPE and 47.5% m-LLDPE/52.5% LDPE samples, owing to their similar σ_M values (Fig. 8).

Notwithstanding the blends which contain a large amount of LDPE show similar melt spinning results, the elongational viscosity of 97.5% m-LLDPE/2.5% LDPE, 95% m-LLDPE/5% LDPE, 92.5% m-LLDPE/7.5% LDPE and 87.5% m-LLDPE/12.5% LDPE blends increases with LDPE concentration (Table 4), due to the presence of long chain branched chains. But the LDPE concentration effect on the 'melt stress' σ_M of these blends is not so evident. Significantly enough, the results of Fig. 8 (where σ_M is given by the maximum σ_{11} reached) lead to contradict the assumption which implies that 'sharkskin' is shifted to higher shear rates as the measured 'melt stress' increases: As can be seen in Table 3 'sharkskin' is considerably postponed in 87.5% m-LLDPE/12.5% LDPE blend as compared to the other blends, although all possess a similar σ_M. Contradictory to this discouraging result, the model of Migler et al., which propose a critical 'reconfiguration rate' for the onset of sharkskin, offers a reasonable explanation for the better performance obtained with 87.5% m-LLDPE/12.5% LDPE blend. As shown in Table 4, this blend possesses the largest elongational viscosity among the m-LLDPE rich blends. We assume that the elongational stress at the exit of the die, which arises from free-fall due to gravity, is similar for these blends. Then the largest η_E of the 87.5% m-LLDPE/12.5% LDPE blend would give rise to lower values of the elongational deformation and the elongational strain rate, which are both proportional to the 'reconfiguration rate' (Eq. (6)). Therefore, since only above a certain critical value of $\dot{T}$ would 'sharkskin' be observed, the reduction of this parameter for 87.5% m-LLDPE/12.5% LDPE blend) would be the cause of the shift of 'sharkskin' to higher shear rates.

Preliminary blown film extrusion experiments performed in a Collin blow film extrusion equipment reveal a larger drawability for m-LLDPE rich blends, than for blends of a higher LDPE content, reducing the thickness of the blown film. But LDPE rich blends stand bigger tensile forces, when the molten polymer tube exiting from the annular die is drawn upward by the take up device, making the film blowing process more reliable and easier to achieve. These general trends are compatible with the melt spinning results, in particular with the plots of the drawdown force F as a function of the drawdown ratio v_1/v_0 (Section 2) displayed in Fig. 9. Larger forces are required to break the strands of LDPE rich blends, but the extensibility (v_1/v_0 at break) is bigger for the blends with a high m-LLDPE content. These results, similar to those reported by Zatloukal et al. [42] and Micic and Battacharya [43], can be useful to improve film blowing process. Interestingly enough the homogeneous melt conditions required for film blow extrusion are not fulfilled for immiscible 47.5% m-LLDPE/52.5% LDPE blend: Despite presenting results similar to LDPE and its miscible blends in melt spinning experiments, is completely unsuitable for blown film extrusion. This is an example of how an immiscible blend with a core-sheet morphology,

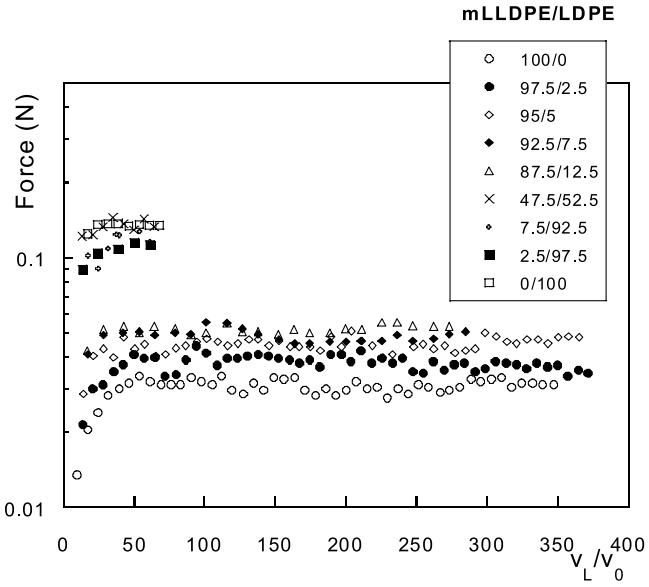

Fig. 9. Plots of the drawdown force F as a function of the drawdown ratio v_1/v_0 (Section 2) for all the samples.

where one of the polymers (LDPE in our case) encircles the other, is able to be processed using methods which require only shear flow, like extrusion, but is unsuitable for more demanding processing techniques. On the other hand, although the effect of the incorporation of long chain branches to m-LLDPE (increasing LDPE content) is noted by a slight enhancement of tensile force in melt spinning experiments (Fig. 9), no difference has been found among m-LLDPE and 97.5% m-LLDPE/2.5% LDPE, 95% m-LLDPE/5% LDPE, 92.5% m-LLDPE/7.5% LDPE and 87.5% m-LLDPE/12.5% LDPE blends in film blowing performance. This result proves the difficulties in the correlation of blown film extrusion performance in industrial equipment, with laboratory experiments, such as extrusion rheometry and melt spinning, beyond the aforementioned general trends.

4. Conclusions

Viscosity results and time–temperature superposition results reveal that all the considered m-LLDPE/LDPE blends, except 47.5% m-LLDPE/52.5% LDPE blend, are miscible in the molten state. Extrusion rheometry results indicate that a core-sheet morphology is developed in the immiscible blend, as the less viscous LDPE encircles the m-LLDPE phase. This morphology explains the similar extrusion and melt spinning results obtained for immiscible 47.5% m-LLDPE/52.5% LDPE blend and miscible 2.5% m-LLDPE/97.5% LDPE and 7.5% m-LLDPE/92.5% LDPE blends. However, the technical limitations caused by immiscibility are made clear in the inability of this two-phase system to blow film extrusion process, which requires a greater melt homogeneity than other processing methods.

Concerning the practical rheological features of the blends with a high m-LLDPE content, the most remarkable result is the shift of the onset of 'sharkskin' to high shear rates, observed for 87.5% m-LLDPE/12.5% LDPE blend. Melt spinning experiments, which allow us to determine an apparent elongational viscosity, as well as the stress at rupture of the melt, are revealed as a suitable technique to investigate 'sharkskin' effect. Based on a recent model developed by Migler et al., we assume that the 'sharkskin' postponing observed for 87.5% m-LLDPE/12.5% LDPE blend is probably due to the elongational viscosity enhancement, associated to the presence of LCB. However, this profitable effect of long chain branched molecules has not been noticed in our blown film extrusion experiments, since m-LLDPE and 97.5 m-LLDPE/2.5% LDPE, 95% m-LLDPE/5% LDPE, 92.5% m-LLDPE/7.5% LDPE and 87.5% m-LLDPE/12.5% LDPE blends show a similar performance.

References

[1] Muñoz-Escalona A, Lafuente P, Vega JF, Muñoz ME, Santamaría A. Polymer 1997;38:589.
[2] Yamaguchi M, Abe S. J Appl Polym Sci 1999;74:3153.
[3] Liu C, Wang J, He J. Polymer 2002;43:3811.
[4] Xu J, Xu X, Chen L, Feng L, Chen W. Polymer 2001;42:3867.
[5] Hameed T, Hussein IA. Polymer 2002;43:6911.
[6] Hussein IA, Hameed T, Sharkh BFA, Mezghani K. Polymer 2003;44:4665.
[7] Hussein IA, Williams MC. Polym Eng Sci 2004;44:660.
[8] Kwag H, Rana D, Cho K, Rhee J, Woo T, Lee BH, et al. Polym Eng Sci 2000;40:1672.
[9] Alamo RG, Londono JD, Mandlekern L, Stehling FC, Wignall GD. Macromolecules 1994;27:411.
[10] Tashiro K, Imanishi K, Izuchi M, Kobayashi M, Itoh Y, Imai M, et al. Macromolecules 1995;28:8484.
[11] Schipp C, Hill MJ, Barham PJ, Cloke VM, Higgins JS, Oiarzabal L. Polymer 1996;37:2291.
[12] Tashiro K, Gose N. Polymer 2001;42:8987.
[13] Mavridis H. J Plast Film Sheeting 2001;17:253.
[14] Ajii A, Sammut P, Huneault MA. J Appl Polym Sci 2003;88:3070.
[15] Wagner MH, Collignon B, Verbeke J. Rheol Acta 1996;35:117.
[16] Bird RB, Amstrong RC, Hassager O. Dynamics of polymer liquids. 2nd ed. New York: Wiley-Interscience; 1987.
[17] Doi M, Edwards SF. The theory of polymer dynamics. Oxford: Clarendon; 1986.
[18] Godshall D, Wilkes G, Krishnaswamy RK, Sukhadia AM. Polymer 2003;44:5397.
[19] Ferry JD. Viscoelastic properties of polymers. 3rd ed. New York: Wiley; 1980.
[20] Ajji A, Choplin L, Prud'homme RE. J Polym Sci, Part B: Polym Phys 1988;26:2279.
[21] Baek DM, Han CD. Polymer 1995;36:4833.
[22] Chuang H, Han CD. J Appl Polym Sci 1984;29:2205.
[23] Han CD, Chuang H. J Appl Polym Sci 1985;30:2431.
[24] Han CD, Chuang H. J Appl Polym Sci 1985;30:4431.
[25] Jauregui B, Muñoz ME, Santamaría A. Macromol Chem Phys 1995;196:3133.
[26] Kapnistos M, Hinrichs A, Vlassopoulos D, Anastasiadis SH, Stammer A, Wolf BA. Macromolecules 1996;29:7155.
[27] Nesarikar AR. Macromolecules 1995;28:7202.

[28] Hagen R, Weiss RA. Polymer 1995;36:4657.
[29] Araujo MA, Stadler R. Makromol Chem 1988;189:2169.
[30] Colby RH. Polymer 1989;30:1275.
[31] Stadler R, Freitas LL, Krieger V, Klotz S. Polymer 1988;29:1643.
[32] Wippler C. Polym Bull 1991;25:357.
[33] Zárraga A, Peña JJ, Muñoz ME, Santamaría A. J Polym Sci, Part B: Polym Phys 2000;38:469.
[34] Han CD, Lem K. Polym Eng Rev 1982;2:135.
[35] Mavridis H, Shroff RN. Polym Eng Sci 1992;32:1778.
[36] Vega JF, Fernández M, Santamaría A, Muñoz-Escalona A, Lafuente P. Macromol Chem Phys 1999;200:2257.
[37] Cogswell FN. J Non-Newtonian Fluid Mech 1977;2:37.
[38] Rutgers R, Mackley M. J Rheol 2000;44:1319.
[39] Migler KB, Lavallée C, Dillon MP, Woods SS, Gettinger CL. J Rheol 2001;45:565.
[40] Migler KB, Son Y, Qiao F, Flynn K. J Rheol 2002;46:383.
[41] Wagner MH, Schulze V, Göttfert A. Polym Eng Sci 1996;36:925.
[42] Zatloukal M, Stach P, Liu P, Saha P. Int Polym Process 2002;17: 223.
[43] Micic P, Bhattacharya SN. Polym Int 2000;49:1580.